IJISET - International Journal of Innovative Science, Engineering & Technology, Vol. 3 Issue 5, May 2016.
www.ijiset.com
ISSN 2348 – 7968

One Pot Synthesis of Silver loaded Mesoporous Silica for Humidity Sensing Applications

Lokesh Malik [*], Nipin Gupta

Department of Electronics and Communication Engineering, Vaish College of Engineering, Rohtak, (Haryana)

Abstract:

One step facile route for the synthesis of silver nanoparticles loaded mesoporous silica via hydrothermal technique has been presented. The incorporation of silver into the silica does not destroy the mesoporous structure. The structural properties were studied by X-ray Diffraction (XRD), Fourier Transform Infrared Spectroscopy (FTIR) and Scanning Electron Microscope (SEM). Comparing with undoped mesoporous silica, Silver-doped mesoporous silica shows improved humidity sensing properties within the relative humidity (RH) range of 11-98%. It shows an excellent linearity, negligible hysteresis and high humidity sensitivity. Besides that it exhibits satisfactory response and recovery time.

Keywords:

Mesoporous silica, silver, XRD, FTIR and SEM

* **Corresponding author:**
E-mail address: surender6561@yahoo.co.in
Tel.: +91- 9813170944.

1. Introduction

The development of porous materials with large specific surface areas is currently an area of extensive research, particularly with regard to potential applications in areas such as catalysis [1], medical diagnosis [2], nano electronic/optical devices [3], sensors [4-5] and nanomaterial

ISSN 2348 – 7968

fabrication [6]. Mesoporous silica developed in 1998, has uniform hexagonal pores with a narrow pore size distribution and a tunable pore diameter of between 5 and 15 nm [7]. The thickness of the framework walls is about 3.1 to 6.4 nm, which gives the material a higher hydrothermal and mechanical stability. Due to robust structures and well-ordered arrays of uniform nanometer-sized channel pores, mesoporous silica materials have been extensively investigated as hard templates for the synthesis of nanoparticles, nanowires, and nanowire networks [6]. The mesoporous silica modification with metal nanoparticles such as Li [8], K [9], Fe [10], Al [11] has been studied because of their unique optical and electronic properties, together with their various applications in fields such as electronics, photonics, catalysts, and nano and biotechnology [2].

In this work, we synthesize Silver loaded mesoporous silica nanocomposite using hydrothermal process and measured its response in 11–98 %RH range. The sensor displays impressively sensitivity along with excellent linearity, negligible hysteresis (~1.2%), quick response time (18 s), rapid recovery time (21.5 s) and stability (1.8%) thereby exposes the role of loading processes in relishing high performance RH sensors.

2. Experimental

2.1 Materials

Tetraethoxy orthosilicate [$(C_2H_5O)_4Si$, TEOS, Sigma Aldrich], Pluronic P123 [$(EO_{20}PO_{70}EO_{20})$, Sigma Aldrich], Silver Nitrate [$AgNO_3$, Fisher Scientific] and other reagents were used as received.

2.2 Preparation of mesoporous silica

Mesoporous silica was synthesized according to the method reported by Li and Zhao [7] using triblock copolymer surfactant Pluronic P123 as structure directing agent. The detailed procedure

ISSN 2348 – 7968

is as follows: 4.2g P123 was first dissolved in 140 ml distilled water at room temperature followed by addition of 25 ml HCl (35%). The mixture was vigorously stirred at 45°C until a homogeneous solution formed under acidic conditions. 9.5 ml of TEOS was then added dropwise to the solution. The resulting mixture was then stirred continuously at 45 °C for 20 hrs. The aqueous solution was then sealed in a Teflon lined stainless steel autoclave and hydrothermally treated at 100 °C for 24 hrs. Subsequently, the autoclave was allowed to cool naturally at room temperature. The products were recovered and washed with deionized water, filtered and then transferred to Petri dishes and evaporated at 80 °C in oven for another 8 hrs. The final samples were calcined at 600 °C for 6 hrs (heating rate 2 °C/min) in air to remove organic templates and thus pure mesoporous silica was recovered.

2.3 Silver-doped mesoporous silica

The silver-doped silica can be synthesized by following the same route as that for pure mesoporous silica with only a difference that $AgNO_3$ was added into the reaction mixture of P123, water and HCl prior to the addition of TEOS. The stirring was done in dark to prevent the reduction of silver. Finally, the calcination of the resultant products also leads to better diffusion of Ag^+ into the mesopores [12].

2.4 Characterization

Mesoporous silica was characterized by a combination of physical techniques. X-ray powder diffraction (XRD) data were acquired on a Bruker D8 advance diffractometer using CuKα monochromatic radiation (λ=1.5418 Å) at 40 kV and 40 mA. Fourier-transform infrared (FTIR) spectra were recorded in the range of 400-4000 cm^{-1} using FTIR spectroscopy (Perkin Elmer-Frontier). The samples were prepared in a pellet form with spectroscopic grade KBr, the thickness of the pallet being about 1.33 mm. Each spectrum was collected at room temperature

ISSN 2348 – 7968

under atmospheric pressure with a resolution of 4 cm^{-1}. Morphology of the samples was characterized by scanning electron micrographs (SEM-EDX, FEI QUANTA 200F) at an acceleration voltage of 10-15 kV. The samples were prepared by distributing the powder samples on a double sided conducting adhesive tape.

3. Results and discussion:

3.1 Characterizations:

The wide angle XRD pattern (2θ= 10°-80°) of pure mesoporous silica and silver doped mesoporous silica composites after calcination are presented in Fig 1. The distinct broad peak centered at 2θ=22° is the characteristic band of amorphous silica walls of the pristine material [13]. In addition to this broad band, four distinct diffraction peaks at 38.1°, 44.2°, 64.3°, and 77° corresponding to (111), (200), (220), and (311) planes of silver (JCPDS no 04-0783) are observed [14]. All the reflections correspond to pure silver metal with face centered cubic symmetry. The high intensity peak for FCC materials is generally (111) reflection, which is observed in our sample. Well resolved characteristics peaks of silver appeared at 2θ= 38.1°, 44.2°, 64.3°, and 77° which can be indexed to cubic reflections of silver.

The FTIR spectra of pure mesoporous silica and silver doped mesoporous silica are shown in Fig 2. The framework bands at 1092, 808 and 464 cm^{-1} are due to asymmetric stretching, symmetric stretching and bend vibrations of Si-O-Si bands, respectively [15]. The broad band around 3430 cm^{-1} can be attributed to surface silanols and adsorbed water molecules. The bands at 2927 and 2854 cm^{-1} are ascribed to asymmetric stretching of C-H species. The bands at 1423 and 1370 cm^{-1} are corresponded to $-CH_2$ and symmetric deformation of $-CH_3$ species [8]. The bands centered around 1635 and 968 cm^{-1} can be connected with the stretching vibrations of the Si-OH group [14]. The incorporation of metal into silica framework has been

ISSN 2348 – 7968

deduced from the changes of band intensity located at 960-970 cm^{-1}, and is assigned to stretching vibration of the Si-O-M (Metal) linkage [16-18]. Due to metal loading in silica framework, the Si-O-H replaces with Si-O-M (Metal).

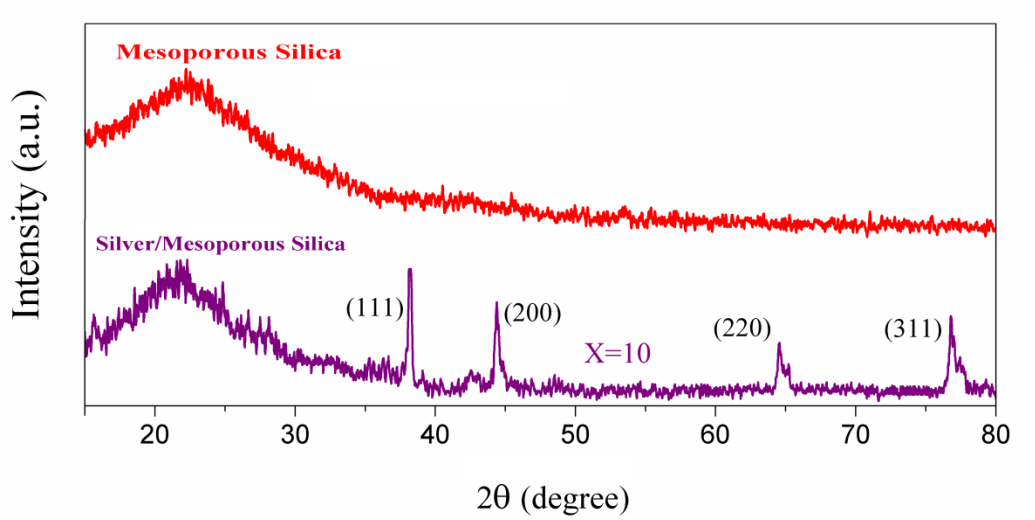

Fig 1: XRD patterns of mesoporous silica and silver doped mesoporous silica composites

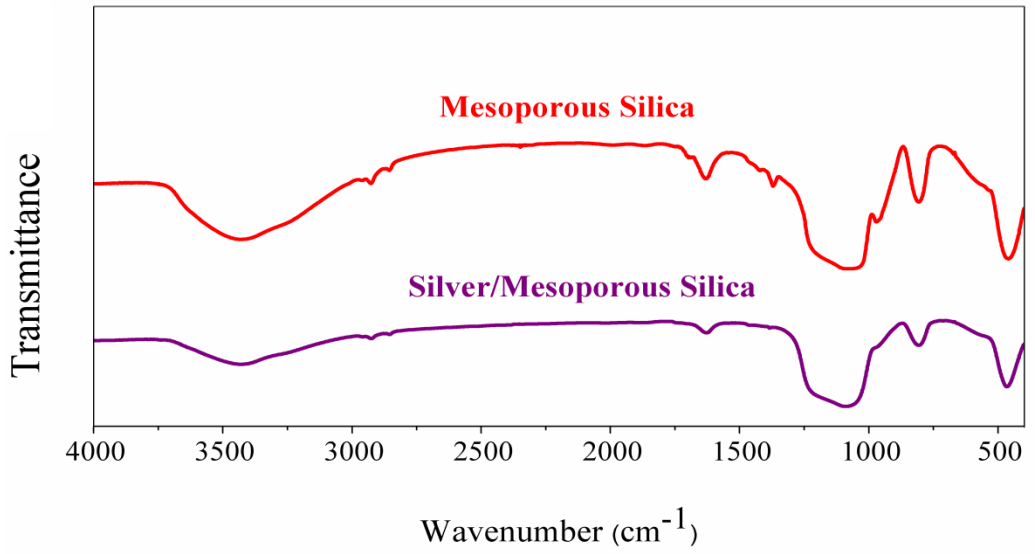

Fig 2: FTIR spectra of mesoporous silica and silver doped mesoporous silica composites

The SEM images of pure mesoporous silica and silver doped mesoporous silica are revealed in Fig. 3(a,b). The mesoporous silica sample consists of short rods with a diameter of

ISSN 2348 – 7968

about 500nm. The morphology of silica is well maintained after incorporation of Ag nanoparticles.

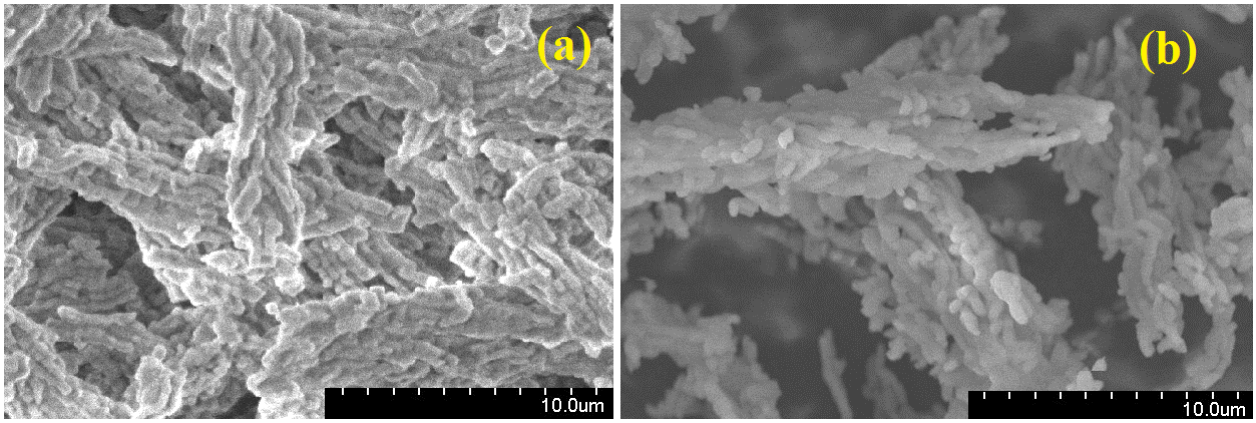

Fig 3: SEM image of (a) mesoporous silica and (b) silver doped mesoporous silica composites

3.2 Humidity sensing properties:

Fig 4(a) shows a 2.5 orders change in impedance measured in 11-98% RH range for pure mesoporous silica-15. Contrarily, silver loaded mesoporous silica exhibits improved RH response which exposes the role of silver nanoparticles in increasing the conductivity and linearity of response for mesoporous silica. Fig 4(b) shows the hysteresis generated in the sensor in the process of adsorption and desorption in the 11-98 %RH range. Hysteresis error was calculated using the equation, $\gamma H = \pm \frac{\Delta H_{max}}{2F_{FS}}$, where, ΔH_{max} is the difference in output of adsorption and desorption processes and F_{FS} is the full scale output. The sensor shows profoundly reversible sensing properties and the sensing curves for the adsorption and desorption process very nearly cover over another, indicating just about immaterial hysteresis. The maximum absolute value of humidity hysteresis error was found to be ~1.2% in 11–98% RH range. This small value of hysteresis indicates the excellent reliability of the sensor.

ISSN 2348 – 7968

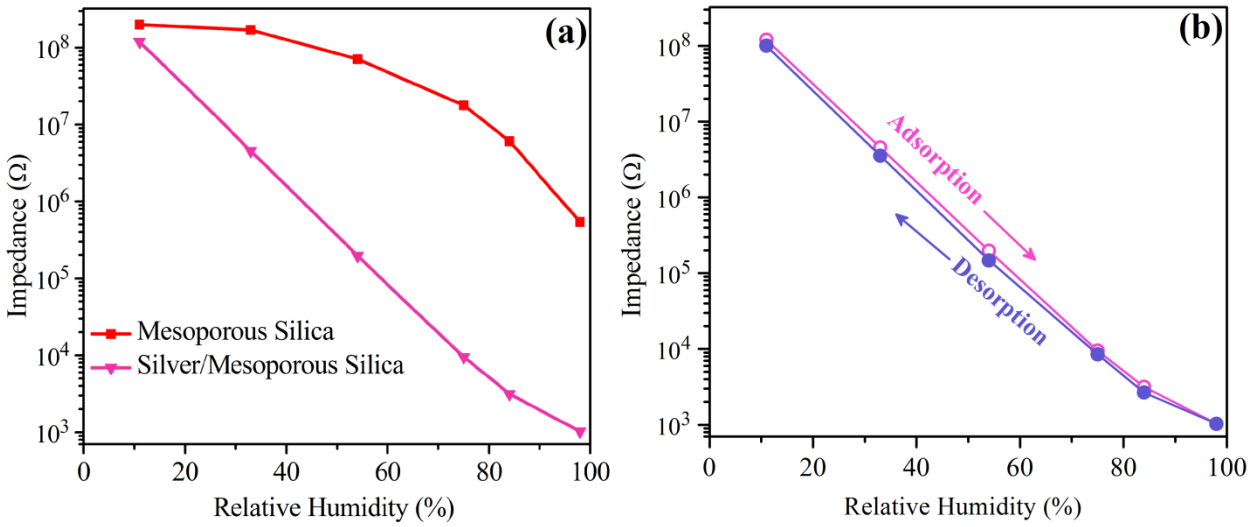

Figure 4: (a) Linearity curves as a function of impedance with %RH and **(b)** Hysteresis of silver doped mesoporous silica nanocomposite

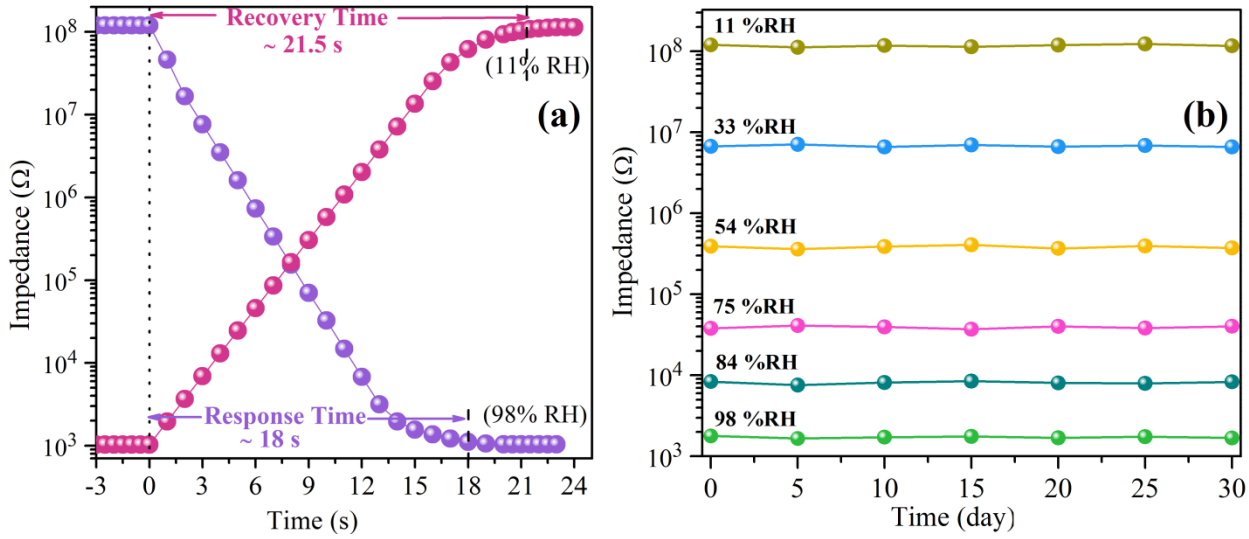

Figure 5: (a) Response/recovery time of silver doped mesoporous silica nanocomposite, **(b)** response monitored at different humidity for 30 days

The performance of silver loaded mesoporous silica was evaluated by measuring the response and recovery time in 11-98 %RH range as shown in Fig 5(a). The comparatively faster adsorption and release of water molecules on the surface/pore channels accounts for relatively quicker response and recovery time. The results shows that the process of humidification and dehumidification is significantly affected due to the presence of open and unblocked pores

ISSN 2348 – 7968

causing smoother transmission of water molecules and charge carriers. To determine the stability of the synthesized sensor, the response towards %RH was tested every 5^{th} day was tested over a span of 30 days. As seen in Fig. 5(b), the sensor shows consistency and a satisfactory variation in impedance (~1.8%) is measured at each humidity level.

4. Conclusion:

In summary, silver doped mesoporous silica nanocomposites with silver nanoparticles loaded in channels and even implanted in frameworks of mesoporous silica have been successful fabricated. The Mesoporous silica is synthesized by nanocasting method in highly acidic conditions using non-ionic surfactant P123 as templating agent. The hydrophobic silver metal nanoparticles are formed simultaneously in this system, and these metallic nanoparticles are inclined to locate in the hydrophobic environment of the inner part of micelles. As a result, the template removal process of calcination will result in silver nanoparticles locating in channels of mesoporous silica materials. This is also confirmed with XRD result which shows peaks only for 0 oxidation state of silver nanoparticles thus confirming that silver is existing inside the silica framework in metallic state. The humidity sensing measurements uncovers the excellent sensitivity of the nanocomposite. Besides the sensor exhibit quick response (18 s) and recovery time (21.5 s), marginal hysteresis (1.2%) and outstanding stability (1.8%) over a span of 30 days in complete 11-98 % RH range. It is believed that RH sensor utilizing mesoporous nanocomposite materials will be effective in outlining materials for novel RH sensing applications.

ISSN 2348 – 7968

References:

1. J. Liu, Q. Yang, M.P. Kapoor, N. Setoyama, S. Inagaki, J. Yang, L. Zhang, J. Phys. Chem. B, 109, 12250–12256 **(2005)**.
2. V. Mamaeva, C. Sahlgren, M. Lindén, Adv. Drug Delivery- Reviews, 65, 689-702, **(2013)**
3. E. Ozkan, S.H. Lee, P. Liu, C.E. Tracy, F.Z. Tepehan, J.R. Pitts, S.K. Deb, Solid State Ionics 149, 139–146, **(2002)**.
4. J. Yang, K. Hidajat, S. Kawi, Mater. Lett. 62, 1441–1443, **(2008)**.
5. C.Y. Liu, C.F. Chen, J.P. Leu, Sensors and Actuators B 137, 700–703, **(2009)**
6. G. Satishkumar, L. Titelman, M.V.Landau, J. Solid State Chem. 182, 2822–2828, **(2009)**
7. D. Zhao, Q. Huo, J. Feng, B.F. Chmelka, G.D. Stucky, J. Am. Chem. Soc. 120, 6024-6036, **(1998)**.
8. T. Zhang, R. Wang, W. C. Geng, X. Li, Q. Qi, Y. He, S. Wang, Sensors and Actuators B, 128, 482–487, **(2008)**
9. W. Zhang, R. Wang, Q. Zhang, J. Li, J. Phys. and Chem. of Solids, 73, 517–522, **(2012)**
10. Q. Qi, T. Zhang, X. Zheng, L. Wan, Sensors and Actuators B 135, 255–261, **(2008)**
11. Y. Li, W.H. Zhang, L. Zhang, Q.H. Yang, Z.B. Wei, Z.C. Feng, C. Li, J. Phys. Chem. B, 108, 9739–9744, **(2004)**.
12. S. Besson, T. Gacoin, C. Ricolleau, Boilot, J. Chem. Commun, 3, 360-361, **(2003)**
13. L.Z. Wang, J.L. Shi, J. Yu, D.S. Yan, Nanostruct Mater, 10, 1289–1299, **(1998)**
14. D.H. Lin, Y. X. Jiang, Y. Wang, S. G. Sun, J. Nanomat., Article ID 473791, **(2008).**
15. S. Vetrivel, A. Pandurangan, J. Mol. Catal. A, 217, 165–74, **(2004)**.
16. X. Zhang, Z. Qu, X. Li, Q. Zhao, X. Zhang, X. Quan, Mat. Lett., 65, 1892–1895, **(2011).**
17. K.S.W. Sing, D.H. Everett, R.A.W. Haul, L. Moscou, R.A. Pierotti, J. Rouquérol, T. Siemieniewska, Pure Appl. Chem. 57, 603-619, **(1985)**.
18. S.Y. Choi, M. Mamak, N. Coombs, N. Chopra, G.A. Ozin, Adv. Funct. Mater. 14 335–344, **(2004).**